# Chapter 5

*Bursting activity in weakly electric fish*

**Rüdiger Krahe[1] and Fabrizio Gabbiani[2]**

[1]Beckman Institute for Advanced Science and Technology and
Department of Molecular and Integrative Physiology
University of Illinois at Urbana/Champaign
405 N. Mathews Ave.
Urbana, IL 61801

[2]Division of Neuroscience
Baylor College of Mecidine
One Baylor Plaza
Houston, TX 77030

## 5.1 Introduction

Neurons in many sensory systems tend to fire action potentials intermittently with spikes grouped into bursts of high-frequency discharge. Functionally, bursts have been implicated in many different phenomena, such as efficient transmission of sensory information [1], regulation of information flow during slow-wave sleep [2], selective communication between neurons [3], epileptic seizures [4], and synaptic plasticity [5]. In recent years, evidence has accumulated that bursts indeed encode sensory information and that they may even be more reliable indicators of important sensory events than spikes fired in tonic mode [1][6][7][8][9][10][11][12]. To understand the biological relevance of bursts and the cellular mechanisms underlying their generation, a wide variety of approaches are needed. *In vivo* recordings from neurons in awake/behaving animals allow investigating how different firing modes affect behavioral performance. *In vitro* experiments, on the other hand, offer a greater control over the preparation and are best suited to study cellular mechanisms of bursting. Finally, various levels of modeling can summarize experimental findings, test our understanding of mechanisms, and inspire new experiments. In this chapter, we will follow this line of investigation and review a number of recent studies of burst firing in weakly electric fish.

The electrosensory system of South American weakly electric fish has proven to be extremely well suited for combined neuroethological and computational studies of information processing from systems neuroscience to the characteristics of ion channels. In this review, we will give a brief introduction to the electrosensory system, describe in more detail the *in vivo* firing properties of electrosensory pyramidal cells in the hindbrain of these fish, and report on the potential behavioral role of bursts. Next, we present results of *in vitro* studies that have elucidated some of the cellular mechanisms underlying burst generation in pyramidal cells. This is followed by a discussion of detailed compartmental models that successfully reproduce *in vitro* bursting and reduced models offering a dynamical systems perspective on burst mechanisms. We conclude by comparing burst firing in weakly electric fish to other systems.

### 5.1.1 What is a burst?

Spike bursts have been described in a large number of systems. Voltage traces from a selection of bursting neurons are displayed in Figures 1 and 5. As is evident from these examples, bursts can occur on a wide range of time scales and vary in their fine temporal structure. Because the biophysical mechanisms underlying bursts can be so diverse, it comes as no surprise that no unique

definition of bursts exists. We will use the term here for the basic event that is part of every burst definition: a burst is a series of action potentials fired in rapid succession, set off in frequency against the rest of a spike train. In an interspike interval (ISI) histogram, burst spikes will typically fall into one peak at short intervals with the rest of the intervals forming either a shoulder to this peak, a low plateau or a second, smaller peak at larger values (Fig.2a) [7][8]. This very general definition has been used in many systems to classify spike sequences as belonging to bursts or not. However, other criteria can be applied as well, as illustrated in Fig.2b-d (see, e.g. [13][14][15][16][17][18][19][20][21][22]). The specific choice of criterion will largely depend on the properties of the system under study.

**Figure 1**

**Examples of spike bursts observed in various preparations. a) The R15 neuron of *Aplysia* generates slow membrane potential oscillations on which bursts of action potentials ride (adapted from [23]). b) Rebound bursts in response to hyperpolarizing current pulses from a depolarizing holding potential in thalamic relay neurons (arrow indicates resting potential; adapted from [24]). c), d) Two types of bursting behavior in cortical neurons of the cat (called intrinsically bursting and chattering cells, respectively; adapted from [25]).**

**Figure 2**

**Examples of criteria used to assign spikes to bursts. a) A dip in the ISI histogram separates burst interspike intervals from longer interburst intervals (arrow; same cell as in Fig.5). b) Joint ISI plots clearly identify initial spikes of a burst (right rectangle) from intraburst spikes (left square; adapted from [9]). c) Bursts may be defined by computing a surprise factor that measures their deviations from the expected patterns of spontaneous independent spikes (adapted from [26]). d) Spike train autocorrelation functions of bursting neurons sometimes show clear peaks that are eliminated by treating bursts as single events (gray line; adapted from [8]). A similar definition has used the power spectrum of spike trains (Fourier transform of the autocorrelation function; see [27]).**

## 5.1.2 Why bursts?

We can now ask in more detail why some nerve cells generate bursts. The answer may not be the same for every cell type, and there may even be different uses for burst firing within the same neuron under different behavioral conditions. At a mechanistic level, evidence has been accumulating that the reliability of synaptic transmission can be significantly enhanced for spikes arriving in rapid succession at the presynaptic terminal [1][28][29][30][12][31]. The physiological consequence of increased transmission probability for burst spikes is noise filtering, where isolated presynaptic spikes can be conceived as noise and bursts as signal [1][32]. Under this scheme, burst firing can improve the reliability of information transmission across synapses. A recent alternative and complementary proposal states that bursts may be a means of selective communication between neurons [3]. If postsynaptic neurons display membrane oscillations with cell-specific frequencies, the interspike intervals within a given presynaptic burst may determine which of the postsynaptic cells will be induced to spike.

But what is it that is signaled by bursts? In the case of relay cells of the lateral geniculate nucleus, it has been shown that bursts as well as spikes generated in tonic mode encode visual information [9]. A current hypothesis states that bursts may signal the detection of objects to the cortex while tonic firing may serve in the encoding of object details [9][10][33]. Another possibility is heightened selectivity of burst spikes compared to isolated spikes as observed in cells in primary auditory cortex that show sharpened frequency tuning for bursts [34]. In section 3 of this chapter we will review recent work on weakly electric fish showing that spike bursts of pyramidal cells at an early stage of electrosensory processing extract behaviorally relevant stimulus features more reliably than isolated spikes.

## 5.2 Overview of the electrosensory system

Electrosensation may seem exotic to us, but it forms an essential part of the sensory world for a number of animal taxa. It allows them to navigate, detect approaching predators and prey, and to communicate (for recent reviews see [35][36]). Furthermore, some of its properties make for interesting comparisons with other, less “exotic”, sensory systems: Similar to the auditory system, the electrosensory system is specialized in processing fast variations in stimulus amplitude and phase. It is quite fascinating that electrosensory processing in fish and auditory processing in barn owls and bats have evolved similar computational algorithms for time coding (e.g., [37][38][39]). The multiple two-dimensional topographical representations of the sensory surface (electroreceptors in the skin of the fish) within the brain are found similarly in

the visual system where there are multiple topographical representations of the retina [40]. Additionally, the principal electrosensory neurons in the hindbrain come as ON- and OFF-types, have center-surround receptive fields, and as in the case of mammalian thalamic neurons (e.g., [10][41][42]), their responses are shaped by descending feedback.

### 5.2.1 Behavioral significance of electrosensation

Electroreception comes in two types, passive and active. The passive sense takes advantage of the electric fields generated by living organisms or, as has been shown in sharks, the electromagnetic field of the earth (e.g., [43]). Unlike passive electrosensation and most other sensory modalities, active electrosensation relies on signals originating from the animal itself. The fish generates an electric field through discharge of an electric organ extending along most of the caudal part of its body (Fig.3). The Gymnotiformes are one of two groups of teleosts that independently evolved active electrosensing [44]. Fish of the two Gymnotiform genera treated here, *Eigenmannia* and *Apteronotus*, produce a quasi-sinusoidal electric organ discharge (EOD) waveform with frequencies between 200 and 1200 Hz, the exact range being species-specific.

Objects or animals with impedance different from that of water perturb the electric field surrounding a fish. Electroreceptors in the skin monitor these distortions and thus provide information about obstacles, approaching predators, or prey (Fig.3; [45][46][47]). Nearby conspecifics also engage in electric communication, for example in the context of courtship [48][49][50]. Thus, the active electrosense allows weakly electric fish to forage and to communicate under conditions when other senses are more or less useless as is the case in their natural habitat: They are nocturnal animals and live in turbid tropical freshwaters, which strongly limits the usefulness of vision. Similar to echolocation in bats, active electrosensation opens an ecological niche that is safe from most diurnal predators. Additionally, it opens a new channel for intraspecific communication.

**Figure 3**

**Objects in the vicinity of a weakly electric fish distort the self-generated electric field. The ensuing change in current flow across the skin - the electrosensory image of the object - is monitored by electroreceptors. a) The sketch is a snapshot of the isopotential lines of the electric field at the peak of an EOD cycle with an object of low conductivity distorting the field. b) Short section of the quasi-sinusoidal EOD waveform of *Apteronotus albifrons* recorded as the potential difference between an electrode next to the head and one close to the tail. c) Sketch illustrating the relationship**

**between amplitude modulation waveform (AM) and the underlying EOD carrier signal.**

## 5.2.2 Neuroanatomy of the electrosensory system

Two sets of primary afferents transmit information on electric field perturbations from electroreceptors in the skin to the first central processing stage in the hindbrain, the electrosensory lateral line lobe (ELL). So-called T-receptor afferents fire strictly phase-locked to each cycle of the EOD, thus carrying information about phase distortions [51]. We will, however, focus on the amplitude-coding pathway that involves a different set of afferents, P-receptor afferents. These nerve fibers fire action potentials in a probabilistic fashion (thus the "P") depending on EOD amplitude (see Figs.3c and 4b). Several thousand P-receptor afferents carry information from all parts of the body to the ELL [52]. There, each individual fiber trifurcates and terminates in three adjoining somatotopic representations of the fish's skin, the centromedial (CMS), centrolateral (CLS), and lateral (LS) segments of the ELL [53] (Fig.4a).

P-receptor afferents directly synapse onto one set of principal output cells of the ELL, the basilar pyramidal cells or E-units ("E-xcited"; Fig.4). The other set of output neurons, the non-basilar pyramidal cells, or I-units ("I-nhibited"), receives indirect feedforward input from the afferents via inhibitory interneurons [54]. Consequently, E-units fire action potentials in response to increases in electric field amplitude, whereas I-units fire in response to decreases [55] (Fig.4b). The spatial receptive fields of pyramidal cells are more complex than their direct connections with primary afferents would suggest: E-units have an excitatory center and an inhibitory surround and vice versa for I-units. This is analogous to ON- and OFF-cells in the visual system [55][56][57][58]. A prominent feature of both types of pyramidal cells is their extensive apical dendrites that extend far into the molecular layer of the ELL (Fig.4a). Here, pyramidal cells receive proprioceptive input and massive feedback from higher centers of electrosensory processing. Descending control via the apical dendrites has been shown to play a role in oscillatory responses of pyramidal cells, in gain control, in shaping receptive field size, in adaptive filtering of predictable sensory patterns, and may also be involved in a sensory searchlight mechanism [59][60][61][62].

## 5.2.3 Electrophysiology and encoding of amplitude modulations

Behaviorally relevant amplitude modulations of the electric field induced by objects, prey, or conspecifics cover a frequency range of up to 80 Hz [63]. With their tonic response properties and firing rates in the range from 50 to 600 spikes per second, P-receptor afferents appear well suited to encode these amplitude modulations by changes in instantaneous firing rate [63][64][65][66] (see Fig.4b). This was confirmed in studies applying linear stimulus-estimation algorithms to the responses of P-receptor afferents to stochastic modulations of electric field amplitude [7][8][67][68][69]. Up to 80% of the stimulus time course can be recovered from single primary afferent spike trains. Therefore, it seems that, prior to entering the hindbrain, electrosensory information is faithfully encoded and undergoes very little processing.

What kind of processing takes place in the ELL? One hypothesis could be that single pyramidal cells perform even better at transmitting detailed information on the stimulus time course than P-receptor afferents by averaging out noise over 5 to 20 primary afferents converging onto them [56][70]. This does not seem to be the case when amplitude modulations are presented over large areas of the body surface, mimicking communication signals. Linear stimulus estimation from pyramidal cell spike trains in *Eigenmannia* yielded poor results compared to primary afferents [7][8][71]. Since neighboring pyramidal cells receive input from overlapping areas of the fish's skin, it is conceivable that the information is conveyed in a distributed manner. However, even when stimulus estimation was based on pairs of spike trains from simultaneously recorded pyramidal cells with overlapping receptive fields, the fraction of the stimulus recovered was still well below the fraction encoded by single primary afferents [71]. Recent studies in the CLS and LS of the related weakly electric fish *Apteronotus leptorhynchus*, however, indicate that pyramidal cells may not act as a homogeneous population in this respect. Bastian and coworkers found that the efficiency for encoding global amplitude modulations scales with the spontaneous firing rate of pyramidal cells (3-50 Hz) [58]. Furthermore, the spatial extent of the stimulus seems to affect how much information a cell can transmit about the amplitude modulations [58]. Thus, it seems possible that a subset of pyramidal cells is able to transmit information on the electric stimulus time course, and that the spatial extent of stimuli affects the response properties, probably via feedback input to the apical dendrites [62]. However, even the best performing cells observed so far do not improve on the performance of P-receptor afferents [7][8][58][67][72].

In summary, compared to the primary afferents, pyramidal cells of the ELL are poor encoders of the stimulus time-course. Hence, the question remains, what kind of information do most ELL pyramidal cells transmit to the next stage of electrosensory processing?

**Figure 4**

**Processing of amplitude modulations of the electric field by P-receptor afferents and pyramidal cells in the ELL. a) P-receptor afferents enter the hindbrain via the octavolateral nerve (VIII) and trifurcate to form three somatotopic maps of the body surface (LS: lateral segment; CLS: centrolateral segment; CMS: centromedial segment). A fourth map (medial segment, MS) is formed by passive electrosensory input, which is not treated here. The cross-section through the hindbrain of *Eigenmannia* shows the layered organization of the ELL maps with the deep neuropil layer (dnl) containing the primary afferent fibers, and the somata of the pyramidal cells forming a distinct dark layer (pyr). Basilar pyramidal cells receive direct input from P-receptor afferents onto their basilar dendrite, while non-basilar pyramidal cells receive indirect inhibitory input via interneurons. In the molecular layer (mol) descending inputs connect onto the apical dendrites of pyramidal cells (adapted from [8]). b) Raster plots of spike trains of P-receptor afferents, E- and I-cells in response to sinusoidal amplitude modulations (top trace).**

## 5.3 Feature extraction by spike bursts

### 5.3.1 Bursts reliably indicate relevant stimulus features

Despite their generally poor performance at encoding the time course of amplitude modulations, inspection of pyramidal cell spike trains shows that their responses are selective (Fig.5). E-units typically fire isolated spikes or short spike bursts in response to upstrokes in stimulus amplitude whereas I-units fire in response to downstrokes. Bursts consist of 2 to 10 spikes with a mean of about 3 spikes per burst. On average, roughly 60% of the spikes fired by a given cell occur in bursts [7]. Spatially extended upstrokes and downstrokes in amplitude are known to be integral parts of the electrosensory input eliciting the so-called “Jamming Avoidance Response” (JAR [73]). In case of the JAR, the signals of two conspecifics interfere, creating a beat pattern extending over a large part of the body. To avoid low-frequency beats, which affect the fish’s ability to electrolocate, nearby animals can actively increase the difference between their EOD frequencies. Localized upward and downward deflections in EOD amplitude moving across the sensory surface, on the other hand, may signal the presence of prey [46]. Thus, global as well as local up- and downstrokes in amplitude are presumably important electrosensory events. It therefore seems plausible that pyramidal cells could signal the occurrence of these temporal stimulus features without transmitting detailed information on the stimulus time course. Various methods are available to quantify neuronal classification performance, for example neural network models that learn the

optimal stimulus pattern eliciting spikes (e.g., [74]). A more direct approach derived from signal detection theory uses a linear operation on the input signal followed by a threshold computation. Thus, the specific issue of interest is whether burst spikes perform better at extracting stimulus features than spikes occurring in isolation.

**Figure 5**

**Pyramidal cells tend to fire spikes in short bursts. Intracellular recording of an I-type pyramidal cell in the CMS stimulated with random amplitude modulations (top trace). Note the coupling of spike bursts and isolated spikes to downstrokes in amplitude (adapted from [8]).**

## 5.3.2 Feature extraction analysis

To quantify how well a spike train discriminates stimulus patterns, one first needs to estimate the optimal stimulus feature for eliciting spikes. Here, we describe the application of a Euclidian pattern classifier to this problem (see [7][8] for a slightly more general method). First, the spike train, x(t), and the stimulus, s(t), are binned so as to allow a maximum of one spike per bin. A variable $r_t$ is defined to take the value 1 if the time bin ending at $t$ contains a spike and the value 0 if it does not contain a spike. Stimulus segments, $\mathbf{s}_t$, ending at time $t$ and comprising ~100 bins prior to time $t$ are assigned to one of two ensembles, P($\mathbf{s}$| r=1) and P($\mathbf{s}$| r=0), depending on whether $\mathbf{s}_t$ preceded a time bin containing a spike or not (i.e., $r_t$=0 or 1; Fig.6). The feature, $\boldsymbol{f}$, is computed from the means, $\boldsymbol{m}_1$ and $\boldsymbol{m}_0$, of these conditional distributions P($\mathbf{s}$| r=1) and P($\mathbf{s}$| r=0): $\boldsymbol{f} = \boldsymbol{m}_1 - \boldsymbol{m}_0$. For E-units, the typical feature is a strong upstroke in stimulus amplitude preceded by a small downstroke (Fig.6 bottom), for I-units it is a strong downstroke preceded by a small upstroke (Fig.7a) [7][8]. It is important to note, however, that the exact shape of the classifier depends not only on the individual cell studied but also on the bandwidth of the stimulus [8]. Typically, only the time bins between 0 ms (spike occurrence) and -300 ms show significant deviations from an amplitude of 0 mV suggesting that pyramidal cells do not integrate over longer time spans of sensory input.

To assess the separation between the two ensembles of stimulus segments, each segment is projected onto the feature vector, $\boldsymbol{f}$, and compared to a threshold value, $\theta$: $h_{f,\theta}(\mathbf{s}) = \langle \boldsymbol{f} ; \mathbf{s} \rangle - \theta$, where $\langle ; \rangle$ denotes the scalar product. The projection, $h_{f,\theta}(\mathbf{s})$, can be conceived of as a measure of similarity between a stimulus segment and the feature vector.

**Figure 6**

**Computation of the Euclidian pattern classifier. For each time bin of a given spike train the stimulus vector preceding this bin is assigned to one of two ensembles (P(s| r=0) and P(s| r=1)) depending on whether the time bin contains a spike or not. The Euclidian classifier is defined as the mean stimulus preceding spikes ($m_1$, right) minus the mean stimulus preceding time bins without a spike ($m_0$, left): $f=m_1-m_0$. For this E-unit, the feature is a strong upstroke in amplitude, peaks at around –25 ms, and then returns to 0 mV. Bandwidth of the stimulus: 0-44 Hz. Adapted from [8].**

The performance of this Euclidian classifier in predicting the occurrence of spikes is quantified using a Receiver Operating Characteristic (ROC) analysis [7][8][75][76]. First, the conditional probability distributions of the projections, $P(h_{f,\theta}(\mathbf{s})|\ r=1)$ and $P(h_{f,\theta}(\mathbf{s})|\ r=0)$, are plotted and compared to threshold, $\theta$ (Fig.7b). A spike is detected if $h_{f,\theta}(\mathbf{s}) > 0$, that is if $\langle f ; s \rangle$ is larger than the threshold (to the right of the dashed vertical line in Fig.7b). Integrating the tail of the distribution $P(h_{f,\theta}(\mathbf{s})|\ r=1)$ to the right of the threshold, $\theta$, yields the probability of correct detection, $P_D$. The right tail of the distribution $P(h_{f,\theta}(\mathbf{s})|\ r=0)$ corresponds to the probability of false alarms, $P_{FA}$. By varying the threshold value, $\theta$, $P_D$ can be determined as a function of $P_{FA}$. The resulting curves are called ROC curves (Fig.7c). The larger the area under a given curve the better is the detection performance. However, false alarms are not the only kind of error that can occur. The second type of error happens when a spike is missed because the corresponding projection value is below threshold ($P(h_{f,\theta}(\mathbf{s})|\ r=1)$ to the left of $\theta$). Therefore, a measure of the misclassification error has to incorporate both, the probability of false alarms and the probability of missed events: $P_E = 0.5[P_{FA} + (1-P_D)]$. The best classification performance of an ideal observer corresponds to the minimum of the plot of $P_E$ versus $P_{FA}$ (Fig.7d).

**Figure 7**

**ROC analysis of feature extraction performance. a) A representative optimal stimulus feature of an I-unit. Bandwidth of the stimulus: 0-12 Hz. b) Probability density distributions of the projections of stimulus segments preceding time bins containing a spike and of stimulus segments preceding time bins without a spike (black curve). Spikes were assigned to two classes, isolated spikes (blue) and burst spikes (red), based on the ISI histogram (Fig.2). The probabilities of correct detection and of false alarms are computed by integrating the tails of the probability distributions to the right of threshold, $\theta$ (dashed vertical line): $P_D=P(\langle f ; s_t \rangle > \theta |\ r_t=1)$, $P_{FA}=P(\langle f ; s_t \rangle > \theta |\ r_t=0)$. c) ROC curves obtained by varying the threshold $\theta$**

**along the abscissa in b. The dashed line indicates chance performance. d) Probability of misclassification, $P_E$, versus probability of false alarm. The best performance of the Euclidian classifier can be read from the minimum of this plot. e) Comparison of feature extraction performance by P-receptor afferents (white bars) and pyramidal cells (black bars). The arrows indicate the respective median values of the two distributions. f) Distributions of the misclassification errors for pyramidal cells from the CMS (black bars) and LS (white bars). a-d adapted from [72]. e and f adapted from [8].**

As is evident from Fig.7b, the probability distribution of stimulus projections for burst spikes is more clearly separated from the distribution of stimuli preceding a spikeless bin than is the one for isolated or all spikes. Consequently, the ROC curve for burst spikes rises more steeply than the one for isolated spikes and all spikes (Fig.7c) yielding the lowest misclassification errors (Fig.7d). The superior feature extraction performance of burst spikes was typical for all cells studied so far in the CMS and LS of the weakly electric fish, *Eigenmannia* (overall 133 pyramidal cells [7][8][71][77]).

When the same analysis was applied to spike trains of primary afferents, they consistently performed worse than pyramidal cells (Fig.7e) [8] suggesting that information is filtered in different ways at the first two stages of electrosensory processing. Feature extraction analysis also revealed differences in performance between cells recorded in different maps of the ELL. Cells from the CMS displayed lower misclassification errors than cells from the LS (Fig.7f) [8]. This finding correlates well with the different behavioral significance attributed to the two maps. The CMS has been shown by lesion experiments [78] to be necessary and sufficient for JAR behavior, which is known to involve the correlation of up- and downstrokes in stimulus amplitude with advances or delays in EOD phase [73]. The LS, on the other hand, was shown to be necessary and sufficient for the processing of electrocommunicatory signals [78], which may involve a more complex analysis of the electrosensory input.

Recently, the analysis of electrosensory information transmission was extended to simultaneously recorded spike trains of pairs of pyramidal cells with overlapping receptive fields [71]. Cross-correlation analysis showed that correlations in spike timing between cells of the same type (two E-units or two I-units) were broad (tens of milliseconds) and were not caused by shared synaptic input, but were induced by the independent coupling of both cells to the stimulus. Feature extraction analysis demonstrated that spikes of two nearby cells occurring within a coincidence time window of 5 to 10 ms significantly improved the reliability of feature extraction compared to burst spikes of the individual neurons (Fig.8b,c). Interestingly, a large fraction of the coincident spikes occurred in bursts (for a coincidence time window of 5 ms, $63\pm15\%$, mean $\pm$ standard deviation; see Fig.8a). This finding supports the thesis that

coincident bursts of spikes may constitute the most reliable neural code [1]. The similar time scales of the typical intraburst interspike interval (10-15 ms) and of the best coincidence time window (5-10 ms) suggest that, from the viewpoint of the postsynaptic target, coincident spikes may be considered as "distributed bursts" (see also [12]).

**Figure 8**

**Feature extraction by distributed bursts. a) Fraction of coincident spikes of two simultaneously recorded I-units from CMS with overlapping receptive fields. Black bars: proportion of spikes of neuron A (left) and B (right) coinciding with spikes on the respective other neuron within the time window displayed on the abscissa. White bars: proportion of coincident spikes that occurred in bursts. Grey bars: overall percentage of spikes that occurred in bursts. b) Left: Minimum probability of misclassification by coincident spikes of neurons A and B as a function of the size of the coincidence time window. Spikes coinciding within a time window of 5-10 ms performed significantly better at feature extraction than did isolated or even burst spikes of the individual neurons (right). c) Summary diagram of feature extraction performance by coincident spikes of pairs of pyramidal cells of the same type (E-E pairs and I-I pairs pooled; n=16), by burst spikes of individual cells, and by isolated spikes of single cells (n=58). Adapted from [71].**

ROC analysis has been applied before to compare signal detection performance by burst and tonic response modes of relay cells in the lateral geniculate nucleus of anesthetized cats [33]. Cells were found to indicate visual stimuli more reliably when firing in burst mode than when in tonic mode. While the role of burst firing in the thalamus remains debated [79][80], evidence is mounting that bursts in thalamic relay cells do occur in the wake animal and that they convey stimulus-related information (reviewed in [10], see also [19][31][81]). It seems, however, that bursts are much less prevalent in thalamic relay cells of awake mammals than they are in pyramidal cells of awake weakly electric fish. Thalamic bursts often appear to be transient responses to the beginning of sensory events, which are then followed by tonic encoding of stimulus details [6][10][82]. In contrast, bursts in electric fish pyramidal cell do not abate over the course of a long stimulus but seem to be the major signaling mode employed by those cells. The feature extraction analysis developed by Gabbiani et al. [7] moves beyond the method employed by Guido et al. [33] by yielding information on the optimal feature driving a given cell and on how reliably the occurrence of this feature is indicated by different subsets of spikes in a spike train.

In conclusion, it appears that, at least for global modulations of stimulus amplitude as used in the studies of weakly electric fish described above, electrosensory information transmission undergoes a dramatic transformation at the earliest stages of processing. The primary afferents reliably encode the stimulus time course by their instantaneous firing rate. At the first central nervous stage of electrosensory processing pyramidal cells extract behaviorally relevant features from the persistent stream of afferent input and indicate their times of occurrence to higher-order nuclei by firing short bursts of spikes and by stimulus-induced coincident activity of groups of cells.

## 5.4 Factors shaping burst firing *in vivo*

As described for other systems [83][84][85][86], the propensity of ELL pyramidal cells to burst is related to their morphology and seems to be under descending control from higher centers of sensory processing. Bastian and coworkers studied spontaneous burst firing by pyramidal cells of the CLS and LS in *Apteronotus leptorhynchus* [87][16]. Spontaneous firing rate of these neurons is negatively correlated with the size of their apical dendrite, whereas the probability to generate spontaneous spike bursts increases with the length of the dendritic arbor. The largest apical dendrites reach high up into the molecular layer of the ELL (Fig.2a) [87][16]. There, the apical dendrites are contacted by parallel fibers originating from the posterior eminentia granularis of the cerebellum [59][60]. These parallel fibers control the spontaneous firing rate of pyramidal neurons as well as their probability to produce spontaneous bursts [16]. They are part of an indirect electrosensory feedback pathway, which is thought to be involved in gain control [60]. Therefore, it is conceivable that this indirect feedback could switch pyramidal cell responses between a bursting and a tonic mode. Firing in burst mode would improve feature extraction performance, whereas in tonic mode pyramidal cells might function as encoders of stimulus time course [16]. Switching between tonic and burst mode, however, has so far not been demonstrated for stimulus-driven pyramidal cell responses. Recent evidence suggests that not only indirect feedback to the dorsal molecular layer but also direct inhibitory feedback to the proximal apical dendrites of pyramidal cells affects their firing patterns [62]. This inhibitory direct feedback pathway supports an oscillatory component of burst responses. It is spatially diffuse and is strongest when amplitude modulations occur over large areas of the body surface as they do when fish engage in electrocommunication. For localized, prey-like stimuli, however, the inhibition is only weak and does not support oscillatory burst responses.

## 5.5 Conditional action potential backpropagation controls burst firing *in vitro*

Slice preparations of the ELL of *Apteronotus leptorhynchus* have proven enormously fruitful in elucidating cellular and network mechanisms of electrosensory processing (reviewed in [60][88]). The laminar organization of the ELL allows for accurate placement of recording and stimulating electrodes in various layers along the pyramidal cell axis (see Fig.4a). Deprived of the natural barrage of primary sensory and feedback inputs, and only stimulated by intracellular constant current injection, pyramidal cells *in vitro* display rhythmic oscillations of the membrane potential, which periodically trigger series of high-frequency spike bursts (30 to over 300 Hz) [88]. The frequency characteristics of this oscillatory burst discharge (burst frequency and intra-burst spike frequency) vary across the three topographic maps of the ELL roughly correlating with pyramidal cell tuning properties observed *in vivo* [57][89][36].

### 5.5.1 Experimental evidence for conditional backpropagation

It was shown early on [90] that active backpropagation of $Na^+$ spikes into the apical dendrite is an integral part of high-frequency burst generation by pyramidal cells, similar to what has been described for several other systems [91]. Spikes are initiated at the soma or axon hillock and travel back into the apical dendrite up to the first major branch points (~200 μm). Membrane depolarization and repolarization in the dendrite are slower than in the soma and therefore dendritic spikes are longer in duration than somatic ones. A fast afterhyperpolarization (AHP) of the somatic membrane increases the potential difference between the soma and the still depolarized dendrite and leads to a sizable amount of current being sourced back into the soma where it supports a depolarizing afterpotential (DAP; Fig.9). In the course of a burst, somatic DAP amplitude is potentiated because of frequency-dependent broadening of dendritic spikes. Consecutive DAPs sum up and cause the frequency of somatic spike generation to increase. Eventually, the DAP itself will reach threshold for spike initiation and a high-frequency somatic spike doublet will be generated (ISI typically < 6 ms). Since the refractory period of the apical dendrite is longer (~4.5 ms) than that of the soma (~2 ms), the dendrite does not support active backpropagation of the second spike of the doublet, and the corresponding DAP at the soma fails allowing the AHP to terminate the burst (Fig.9b). This mechanism of burst generation and termination has been termed “conditional backpropagation” [92], because backpropagation is essential for burst production, and it is conditional on sufficiently low spike frequencies. When

spike frequency exceeds the dendritic refractory period, backpropagation fails and the burst is terminated.

A number of cellular components of the burst mechanism have been identified. $Na^+$ channels are distributed in a punctate manner along the proximal 200 μm of the apical dendrite consistent with the finding that active backpropagation of TTX-sensitive spikes terminates at about this distance from the soma [90]. A candidate mechanism for the broadening of dendritic spikes is cumulative inactivation of a dendritic $K^+$-conductance [92]. The inactivation would slow the repolarization of the dendritic membrane potential in a spike-frequency-dependent manner, thus increasing the amplitude of the somatic DAP. A likely candidate for this current is the Apteronotid homologue of the mammalian Kv3.3 $K^+$-channel (*Apt*Kv3.3), which is extensively distributed along the entire axis of pyramidal cells [93][94]. Local blockade of dendritic *Apt*Kv3.3 led to slowing of spike repolarization and increase in somatic DAP with a time-course similar to that of a regular burst. This manipulation also lowered the threshold for burst discharge evoked by current injection into the soma [94]. Therefore, it seems likely that this high-voltage-activated $K^+$ channel is either directly involved in the mechanism of burst discharge or at the very least can modulate the threshold for burst generation [95]. Another contribution to the potentiation of the somatic DAP in the course of a burst comes from a persistent $Na^+$ current which is activated by the increasing dendritic spike duration [96]. In contrast to other systems (for review see [97]), $Ca^{2+}$ currents or $Ca^{2+}$-dependent $K^+$ currents do not appear to be necessary for burst generation in this system [92][96][95].

The detailed knowledge of pyramidal cell morphology, the organization of primary sensory and feedback input, and of the conductances shaping burst firing *in vitro*, makes pyramidal cells ideally suited for detailed modeling of the mechanism underlying burst firing. This mechanism differs in interesting ways from burst generation as described in several other systems. One obvious peculiarity of ELL pyramidal cell bursts is that ISI duration decreases in the course of a burst (Fig.9b), a phenomenon that has not been described in any other system so far. *In vivo*, however, this ISI pattern can be observed only rarely (Krahe, unpublished observations). With natural synaptic input, other factors like inhibition and the interplay between afferent and feedback input may also shape the bursts and contribute to their termination. Furthermore, the basilar dendrites of E-units warrant closer investigation since they have been shown to be equipped with $Na^+$ channels as well as *Apt*Kv3.3 $K^+$ channels, and might thus also support backpropagation and bursting in a way similar to the apical dendrite [90][93][94] (see also [98] for similar conclusions in neocortical pyramidal neurons).

**Figure 9**

**Summary of the mechanism underlying high-frequency burst generation in pyramidal cells *in vitro*. a) Schematic diagram of a pyramidal cell with a narrow spike recorded in the soma (1). The somatic spike is actively propagated back into the apical dendrite where a much broader version of the same spike can be recorded (2). Current sourcing from the dendrite back into the soma causes a DAP (3). b) Top: Oscillatory burst discharge recorded in the soma of a pyramidal cell with 0.74 nA depolarizing current injection. Middle and bottom: Somatic and dendritic spike burst recorded separately in two different cells. The time scales are adjusted to allow alignment of spikes. Somatic spikes are truncated. As evident from the dendritic recording, spike repolarization slows down in the course of a burst allowing the DAP at the soma to potentiate. Eventually, the DAP reaches threshold and causes a high-frequency spike doublet. Since the dendritic refractory period is longer than the somatic one, the dendrite cannot support active propagation of the second spike of the doublet. The DAP fails and allows the afterhyperpolarization (AHP) to terminate the spike burst. a adapted from [92], b adapted from [96].**

### 5.5.2 Multicompartmental model of pyramidal cell bursts

Based on the detailed spatial reconstruction of a dye-filled E-type pyramidal cell [99], Doiron et al. [96][100] developed a multicompartmental model that successfully reproduces burst firing as it is observed *in vitro* (Fig.9). The main goal of these studies was to identify the components of the burst mechanism that underlie dendritic spike broadening and somatic DAP potentiation since those are responsible for the progressive decrease in ISI duration and eventual burst termination. A key feature of the model was the presence of fast $Na^+$ and $K^+$ currents in both somatic and dendritic compartments, to account for $Na^+$ action potential generation and backpropagation (Fig.10a). In order to achieve the narrow somatic and broader dendritic spike shapes (see 5.5.1), the time constants of the active conductances in the dendrite had to be increased relative to the soma. This also yielded a relatively longer refractory period for the dendritic spike compared to the somatic one.

While the core model outlined above reproduced key features of the somatic and dendritic response, it failed to generate spike bursts. Doiron et al. [100] were able to exclude a number of potential burst mechanisms described for other systems: $Ca^{2+}$- or voltage-dependent slowly activating $K^+$ channels, slow inactivation of the dendritic $Na^+$ channel, and slow activation of the persistent $Na^+$ current. Finally, modification of the dendritic delayed rectifier channel yielded burst properties corresponding to the *in vitro* findings: A low-threshold slow inactivation of the $K^+$ conductance led to dendritic spike broadening in the

course of a burst and to a corresponding increase in the DAP amplitude, which eventually triggered a doublet, leading to dendritic spike failure and burst termination due to the AHP. Whereas slow activation of the persistent $Na^+$ current proved insufficient to elicit proper bursting, it was recently shown to be an important component of the DAP potentiation [96]. It is activated by the broadening of dendritic spikes and boosts the sub-threshold depolarization of the somatic membrane. Thereby it largely determines the time it takes to reach threshold for doublet firing. Since the doublet terminates the burst, the persistent $Na^+$ current thus controls burst duration. With the interburst period being largely fixed by the duration of the AHP, the persistent $Na^+$ current also determines burst oscillation period [96]. Since it can be activated by descending feedback to the apical dendrites [99][101], this provides a potential mechanism for controlling burst firing depending on behavioral context.

To summarize, the key features of the pyramidal cell burst mechanism are i) a dendritic $Na^+$ conductance that supports active backpropagation of spikes into the dendrite and that feeds the somatic DAP, ii) a slow cumulative inactivation of a delayed rectifier current which leads to dendritic spike broadening in the course of a burst, thus potentiating the somatic DAP, iii) a shorter refractory period for somatic spikes compared to dendritic ones renders backpropagation conditional on the instantaneous firing rate, iv) the rate of the DAP potentiation, which is part of a positive feedback loop in which dendritic spike broadening activates a persistent $Na^+$ current, which further boosts depolarization. The slow dynamics of the persistent $Na^+$ current largely control burst duration and burst frequency.

**Figure 10**

**Multi-compartmental model of burst generation. a) The model was based on the detailed reconstruction of a dye-filled E-type pyramidal cell [99]. The distribution of ionic channels along the neuron's axis is indicated in the insets. The detailed placement of $Na^+$ and $K^+$ channels in separate compartments of the proximal dendrite is shown on the left. b) The model reproduces the increasing firing frequency in the course of a burst with a doublet at the end and a burst AHP (top). The dendritic delayed-rectifier conductance, $g_{Dr,d}$ , shows cumulative inactivation as the burst evolves (middle). The dendritic voltage-gated $Na^+$ conductance, $g_{Na,d}$ , fails when the somatic ISI is within its refractory period (bottom). c) Summary graph showing the decrease in peak conductance of $g_{Dr,d}$ and $g_{Na,d}$ as a function of spike number for the burst shown in b. Whereas $g_{Dr,d}$ inactivates in a cumulative way, $g_{Na,d}$ decays much more gradually but is completely shut off by the high-frequency doublet. Adapted from [100].**

### 5.5.3 Reduced models of burst firing

Detailed biophysical models are powerful tools for probing the understanding of cellular mechanisms at a microscopic scale. However, they are computationally too complex for modeling of large networks or for analyzing the behavior of single cells from a dynamical systems perspective. Having understood the key mechanisms, it is often possible to reduce a detailed biophysical model to its essential components and then apply dynamical systems analysis to the lower-dimensional model [102]. The multi-compartmental model described above has undergone two such reductions, first to a two-compartment model, termed a "ghostburster" for reasons explained in more detail below [103], and then to an even simpler two-variable delay-differential-equation model [104].

To model the generation of the somatic DAP, only a somatic and one dendritic compartment representing the entire apical dendritic tree are needed (Fig.11a) [103]. Soma and dendrite were equipped with fast $Na^+$ channels, delayed rectifier $K^+$ currents, and passive leak current. Current flow between the compartments followed simple electrotonic gradients determined by the coupling coefficient between the two compartments, scaled by the ratio of somatic to total model surface (see also [29][86][105]). Thus, the entire system was described by only six nonlinear differential equations using modified Hodgkin/Huxley kinetics [106]. To achieve the relatively longer refractory period of the dendrite [92], the time constant of dendritic $Na^+$ inactivation was chosen to be longer than somatic $Na^+$ inactivation and somatic $K^+$ activation. The key element for the burst mechanism was the introduction of a slow inactivation variable for the dendritic delayed rectifier current, whose time constant was set to about 5 times slower than the mechanisms of spike generation. In this configuration, the two-compartmental model reliably reproduced the potentiation of the somatic DAP, which eventually triggers the firing of a spike doublet, the burst termination due to failure of backpropagation, and the rapid onset of the AHP [103] (see Fig.9b).

To study the burst dynamics, the ghostburster model was treated as a fast-slow burster [102][107], separating it into a fast subsystem representing all variables related to spike generation, and a slow subsystem representing the dendritic $K^+$ inactivation variable, $p_d$. The fast subsystem could then be investigated using the slow variable as a bifurcation parameter. The dashed lines in Figure 11b show the quasi-static bifurcation diagram (dashed line) with maximum dendritic membrane voltage as a representative state variable of the fast subsystem, and $p_d$ as the slow subsystem. For constant values of $p_d > p_{dl}$, there exists a stable period-one solution. At $p_d = p_{dl}$ the fast subsystem transitions to a period-two limit cycle. This corresponds to intermittent doublet firing with dendritic spike failure, since for $p_d < p_{dl}$ dendritic repolarization is sufficiently slow to cause very strong somatic DAPs capable of eliciting a second somatic spike after a

small time interval (~ 3 ms). The overlaid burst trajectory (solid line) shows the beginning of the burst on the right side (upwards arrow). The maximum of the dendritic membrane voltage decreases for the second spike of the doublet (compare Fig.9b), which occurs at $p_d < p_{d1}$. The short doublet ISI is followed by the long interburst ISI, the slow variable recovers until the next burst begins. Because $p_d$ is reinjected near an infinite-period bifurcation (saddle-node bifurcation of fixed points responsible for spike excitability), Doiron et al. [103] termed this burst mechanism "ghostbursting" ("sensing" the ghost of an infinite-period bifurcation [108]). Thus, the two-compartment model nicely explains the dynamics of pyramidal cell bursting observed in vitro by the interplay between fast spike-generating mechanisms and slow dendritic $K^+$-channel inactivation.

**Figure 11**

**Two-compartment model of burst generation. a) Sketch of the somatic and dendritic compartments linked by an axial resistance. b) The dashed lines show the quasi-static bifurcation diagram with a representative of the fast subsystem, the maximum dendritic membrane voltage, as a function of the slow subsystem, the dendritic $K^+$ inactivation variable, $p_D$. Overlaid is a single burst trajectory (solid line; burst begins with the upwards pointing arrow on the right). Adapted from [103].**

In a further reduction of the model, Laing and Longtin [104] replaced the six ordinary differential equation model by an integrate-and-fire model consisting of a set of two discontinuous delay-differential equations. An interesting aspect of this model is that it uses a discrete delay to mimic the ping-pong effect between soma and dendrite. When a spike occurs, the somatic membrane potential is boosted by a variable amount but only if the preceding ISI was longer than the dendritic refractory period and only after a certain delay. The amount of somatic boosting depends on the firing history of the neuron. For long ISIs, it decays towards zero, for short ISIs it builds up.

Bifurcation analysis of both the ghostburster and the delay model revealed properties that contrast with other models of burst generation. When increasing amounts of current are injected into the soma, both reduced models move from quiescence for subthreshold current through a range of tonic periodic firing into irregular bursting (Fig.12) [103][104]. The transition from quiescence to tonic firing is through a saddle-node bifurcation of fixed points after which the systems follow a stable limit cycle. The periodic attractor increases monotonically in frequency as current is increased. The fact that the models pass from quiescence to repetitive firing through a saddle-node bifurcation is characteristic of class I excitability [102][107]. Accordingly, the neurons are able to fire at arbitrarily low rates close to the bifurcation, which is also

observed when injecting small amounts of current into pyramidal cells in the slice preparation [92]. At higher current the models move through a saddle-node bifurcation of limit cycles after which they follow a chaotic attractor corresponding to burst firing. For very large input currents, the cells periodically discharge spike doublets (right of the dotted line in Fig.12 a, b). This progression from quiescence through periodic firing and bursting to periodic doublet discharge closely reproduces the behavior of pyramidal cells in the slice preparation [92]. Similar to the ghostburster model, the delay integrate-and-fire model also allows the generation of a wide 'gallery' of bursts of different shapes indicating that pyramidal cells may be able to adjust burst duration and frequency depending on context.

The simplicity of the delay model also allowed examination of the effects of periodic forcing corresponding to injection of sinusoidal current at the soma. Depending on the frequency of sinusoidal forcing, the threshold for burst firing could be increased or decreased relative to the threshold in the unforced system. This finding suggests that depending on the frequency of amplitude modulations of the electric field, the threshold for burst firing of pyramidal cells might shift.

The most appealing aspect of the delay model is its simplicity and computational efficiency. Since the model captures the basic properties of burst firing described by the more elaborate ionic models [100][103], it may be suitable for use in larger-scale models of electrosensory processing.

**Figure 12**

**Instantaneous firing frequency versus amount of injected current for a) ghostburster model, and b) two-variable delay-differential-equation model. Both models show an absolute threshold for firing, above which they discharge periodically. At some intermediate current ($I \sim 8.5$ for the ghostburster model and $I \sim 1.22$ for the delay model), the models transition through a saddle-node bifurcation of limit cycles into irregular bursting. At very high input currents they begin to fire doublets (right of the dotted line in a and b). Doublet firing involves two distinct ISI values, the long inter-doublet ISI (upper line) and the short doublet ISI (lower line). a adapted from [103], b adapted from [104].**

## 5.6 Comparison with other bursting neurons

Bursting neurons have been described in a variety of systems including the crustacean stomatogastric ganglion [109], the lamprey spinal cord [110], dorsal

root ganglion cells [111], thalamic reticular and relay cells [2][10], and pyramidal neurons in several cortical areas and layers [25][84][85]. Naturally, the depth of understanding of the underlying ionic mechanisms is not the same for every system. However, modeling approaches based on experimental findings have been helpful in elucidating cellular and dynamical aspects of burst firing in a number of different preparations. In the following, we discuss three aspects of burst firing to which the electric fish preparation has brought new perspectives: 1) burst firing can be caused by a "ping-pong" interplay between soma and dendrite. 2) ghostbursting offers novel dynamics for oscillatory bursting. 3) the underlying ionic mechanisms shape the ISI sequence within the burst.

### 5.6.1 "Ping-pong" between soma and dendrite

The term "ping-pong" [29] refers to the interplay between soma and dendrite that has been shown to be an essential part of the burst mechanism in a number of cell types. The idea that soma-dendritic interactions shape neuronal response properties became prominent when intracellular labeling and electrophysiology were combined (e.g., [85][112]). Based on reconstructions of various neocortical cell types, Mainen and Sejnowski [86] showed that neurons sharing the same ionic channel distributions but differing in dendritic morphology displayed a wide range of response properties from regular firing to rhythmically bursting. Dendritic $Na^+$ channels proved to be necessary for bursting since they support backpropagation of spikes into the dendrite and the subsequent current flow back into the soma. The somatic DAP can then feed further spikes, similar to the mechanism described above for ELL pyramidal cells [92][100]. Two basic mechanisms for boosting the DAP seem to be realized in bursting neurons. First, voltage-activated dendritic $Ca^{2+}$ channels have been found to increase the somatic DAP in pyramidal cells in layer 5 of neocortex [30][113], in the subiculum [114] and at least in a fraction of CA1 pyramidal cells of the hippocampus [115][116]. Second, the somatic DAP can be enhanced by persistent $Na^+$ currents as observed in cortical chattering cells [117], in layer 3 sensorimotor cortical neurons [118], some hippocampal CA1 neurons [119][120], and in ELL pyramidal cells [96]. In these latter cases, $Ca^{2+}$ has been shown not to be a necessary component for bursting. Wang [29] suggested that spike-triggered $Ca^{2+}$ influx might be too slow to support bursting at high $\theta$-frequencies (20-70 Hz) observed in chattering cells [25][117][121]. The same reasoning could apply to bursting of ELL pyramidal cells *in vitro*, which shows oscillations in the $\theta$-range [89][90], and which is $Ca^{2+}$-independent [92].

These systems all share a somatic DAP induced by current flow from the dendrite. They differ, however, in several other aspects such as, for example, mechanisms of burst termination. In layer 3 cells of sensorimotor cortex, $Ca^{2+}$-activated $K^+$ channels repolarize the dendrite and stop the current flow towards

the soma [118]. This mechanism had been predicted by a multi-compartmental modeling study of layer 5 intrinsically bursting pyramidal cells [98]. Based on a two-compartment model of neocortical chattering cells, Wang [29] suggested that bursts are terminated when a dendritic voltage-dependent $K^+$ channel is sufficiently activated to repolarize the dendritic membrane. Hence, the above described burst termination by failure of backpropagation due to the relatively long dendritic refractory period constitutes a hitherto unknown mechanism [92].

For thalamic relay cells it was long believed that dendrites did not play a major role in burst generation since bursting persists in acutely isolated cells devoid of dendrites [97]. In a recent combined *in vitro* and modeling study, however, Destexhe and coworkers showed that the low-threshold $Ca^{2+}$ channels underlying burst generation had to have a roughly 5 times higher density in the dendrite than in the soma to yield $Ca^{2+}$ spikes comparable to those seen in intact relay cells [122]. The actual burst consists of fast $Na^+$ and $K^+$ activity riding the crest of the $Ca^{2+}$ spike. At depolarized membrane potentials, the underlying $I_T$ channel is inactivated and the cells respond in tonic mode [10]. Deinactivation requires hyperpolarization for at least 50-100 ms. Therefore, thalamic bursting is characterized by very long ISIs preceding the actual burst.

It should be mentioned that soma-dendritic interactions are not the only route to bursting. Some cell types, such as cerebellar granule cells, seem to be electrotonically too compact to support a ping-pong mechanism [86][123]. Instead, a persistent $Na^+$ current in conjunction with a slow $Ca^{2+}$-independent $K^+$ current can cause oscillations, with fast $Na^+$ spikes riding on top of the oscillations [123].

### 5.6.2 Dynamical properties of burst oscillations

On a more macroscopic scale, bursting in ELL pyramidal cells seems unique in two respects. First, ISI duration decreases within bursts, which is atypical. Second, the changes in firing properties with increasing input current exhibit an unusual bifurcation structure. As shown in the slice preparation [92] and in both the reduced models [103][104], the firing properties pass from quiescence for subthreshold input current through tonic firing for intermediate current levels to bursting. Other systems, in contrast, have been shown to pass from quiescence through bursting to tonic firing (e.g. [2][25][29][98][113][123][124][125]). Accordingly, for a given input current, bursting systems are usually described as switching between quiescence (fixed point) and spiking (limit cycle) [107]. As shown by the reduced ELL pyramidal cell models, however, the fast subsystem can always follow a limit cycle [103][104]. Since the slow subsystem is itself oscillating, it modulates the period of the fast subsystem and forces it to pass near the ghost of an infinite-period bifurcation, which yields the long interburst intervals, as opposed to bifurcating to a fixed point solution.

### 5.6.3 Intra-burst ISI sequences

Within a burst fired by an ELL pyramidal cell, instantaneous firing rate increases until a spike doublet eventually terminates the burst. Due to its long refractory period, the dendrite fails to actively backpropagate the action potential allowing the AHP to set in and repolarize the soma (Fig.9b). From a dynamical systems point of view, the burst termination can be understood as a bifurcation from a period-one to a period-two limit cycle of the fast, spike-generating, system (Fig.11b). In all other models of bursting neurons, bursts end with a transition form a period-one limit cycle to a fixed point (quiescence; [107]). This corresponds to the observation that, in most systems, bursts begin with a very high instantaneous firing rate and then slow down. One reason for the slow-down can be the gradual activation of a dendritic $K^+$ channel which reduces current flow to the soma and increases the time to reach threshold for action potential firing [29][98][118]. Alternatively, spike backpropagation, and with it the somatic DAP, can fail when dendritic $Na^+$ channels cumulatively inactivate [114][126][127] or when synaptic inhibition sufficiently hyperpolarizes the dendritic membrane [128][129][130].

## 5.7 Conclusions

Two main lines of evidence indicate that bursts can play an important role in neuronal information transmission. First, bursts have been shown to surpass single spikes in their information carrying performance [7][8][9][33][34]. Besides acting as unitary events, burst duration, that is the number of spikes, may also be a mode of information transmission [14][131]. Second, high-frequency burst firing increases the reliability of synaptic transmission at unreliable synapses [1][12][28][29][30][31]. The development of the technique of feature extraction analysis has given us a powerful tool to quantify how reliably neurons indicate the occurrence of certain stimulus features without prior knowledge of what these features look like [7][8][72]. Its application to neuronal responses in various behavioral contexts may teach us how the possible contribution of burst firing (or other firing patterns) to information transmission changes with changing behavioral context.

Compartmental modeling based on detailed reconstructions of neuronal morphology has demonstrated that dendritic structure is a major determinant of a neuron's firing properties [84][85][86][91][132]. From a mechanistic point of view, reduced models, such as two-compartment models and point neurons, have been effective at revealing the underlying dynamics of burst generation. As

illustrated here, detailed multi-compartmental modeling can aid in understanding the ionic and structural mechanisms underlying particular neuronal firing patterns [96][100] and, when that is achieved, simplified models can help in elucidating the dynamic properties of these mechanisms [103][104]. The ghostburster model and the delay model reproduce burst discharge as it is observed *in vitro* in spite of their simplicity, suggesting that the essential components of the intrinsic burst mechanism are understood.

For pyramidal cells in the ELL of weakly electric fish, there are first indications that the probability of burst generation is under descending control and depends on the spatial geometry of the stimulus [16][62][92][94]. Similar observations have been made for thalamic neurons (e.g., [10][17][42]) and nerve cells in the subthalamic nucleus [21]. Modeling studies will be key in the exploration of how descending control shapes burst firing. Interestingly, ELL pyramidal cells possess a number of spatially distinct input areas that could be controlled separately depending on behavioral context [59][60].

One of the most urgent questions to be addressed is whether or not the mechanisms that shape bursting under *in vitro* conditions are also the key determinants of burst firing in the intact animal. Of course, the ionic channels responsible for conditional backpropagation will be at work *in vivo*, too. Nevertheless, most pyramidal cells when recorded *in vivo* do not show shortening of ISIs in the course of a burst, at least under the stimulus conditions studied so far [7][8][16]. The models described above therefore need to be refined. They need to address the effects of naturalistic synaptic input from the sensory afferents, including the effects of indirect inhibitory input via local interneurons, and the possible contributions of descending control. Descending control could act directly via synaptic excitation and inhibition, but also indirectly by modulations of synaptic transmission [59] or by inducing phosphorylation of the *AptKv3.3* $K^+$ channel [94]. The development of the reduced models may also make it possible to construct larger network models that could still incorporate naturalistic spike train statistics. Two construction blocks for such a network model could be the delay-differential equation model of an ELL pyramidal cell [104] and a recently developed simple model of P-receptor afferents that captures much of the experimentally observed firing dynamics [133].

## 5.8 Acknowledgments

We gratefully acknowledge the very generous provision of figure material by Ray Turner and Brent Doiron. We also would like to thank Ling Chen for help

with Figures 3A and 12b, and Mark Nelson and Brent Doiron for critically reading the manuscript. The work on stimulus encoding and feature extraction in the electrosensory system was a collaboration with Walter Metzner, Gabriel Kreiman, and Christof Koch, and was supported by NSF.

## 5.9 References

[1] Lisman JE (1997) Bursts as a unit of neural information: making unreliable synapses reliable. Trends Neurosci 20:38-43.

[2] Steriade M, McCormick DA, Sejnowski TJ (1993) Thalamocortical oscillations in the sleeping and aroused brain. Science 262:679-685.

[3] Izhikevich EM (2002) Resonance and selective communication via bursts in neurons having subthreshold oscillations. BioSyst 67:95-102.

[4] McCormick DA, Contreras D (2001) On the cellular and network bases of epileptic seizures. Annu Rev Physiol 63:815-846.

[5] Paulsen O, Sejnowski TJ (2000) Natural patterns of activity and long-term synaptic plasticity. Curr Opin Neurobiol 10:172-179.

[6] Guido W, Weyand T (1995) Burst responses in thalamic relay cells of the awake behaving cat. J Neurophysiol 74:1782-6.

[7] Gabbiani F, Metzner W, Wessel R, Koch C (1996) From stimulus encoding to feature extraction in weakly electric fish. Nature 384:564-567.

[8] Metzner W, Koch C, Wessel R, Gabbiani F (1998) Feature extraction by burst-like spike patterns in multiple sensory maps. J Neurosci 18:2283-2300.

[9] Reinagel P, Godwin D, Sherman SM, Koch C (1999) Encoding of visual information by LGN bursts. J Neurophysiol 81:2558-2569.

[10] Sherman SM (2001a) Tonic and burst firing: dual modes of thalamocortical relay. Trends Neurosci 24:122-126.

[11] Martinez-Conde S, Macknik SL, Hubel DH (2002) The function of bursts of spikes during visual fixation in the awake primate lateral geniculate nucleus and primary visual cortex. Proc Natl Acad Sci USA 99:13920-13925.

[12] Usrey WM, Alonso J-M, Reid RC (2000) Synaptic interactions between thalamic inputs to simple cells in cat visual cortex. J Neurosci 20:5461-5467.

[13] Lu SM, Guido W, Sherman SM (1992) Effects of membrane voltage on receptive field properties of lateral geniculate neurons in the cat: contributions of the low-threshold $Ca^{2+}$ conductance. J Neurophysiol 68:2185-98.

[14] DeBusk BC, DeBruyn EJ, Snider RK, Kabara JF, Bonds AB (1997) Stimulus-dependent modulation of spike burst length in cat striate cortical cells. J Neurophysiol 78:199-213.
[15] Ramcharan EJ, Gnadt JW, Sherman SM (2000) Burst and tonic firing in thalamic cells of unanesthetized, behaving monkeys. Visual Neuroscience 17:55-62.
[16] Bastian J, Nguyenkim J (2001) Dendritic modulation of burst-like firing in sensory neurons. J Neurophysiol 85:10-22.
[17] Fanselow EE, Sameshima K, Baccala LA, Nicolelis MA (2001) Thalamic bursting in rats during different awake behavioral states. Proc Natl Acad Sci USA 98:15330-15335.
[18] Jung H-Y, Mickus T, Spruston N (1997) Prolonged sodium channel inactivation contributes to dendritic action potential attenuation in hippocampal pyramidal neurons. J Neurosci 17:6639-6646.
[19] Weyand TG, Boudreaux M, Guido W (2001) Burst and tonic response modes in thalamic neurons during sleep and wakefulness. J Neurophysiol 85:1107-1118.
[20] He J, Hu B (2002) Differential distribution of burst and songle-spike responses in auditory thalamus. J Neurophysiol 88:2152-2156.
[21] Urbain N, Rentero N, Gervasoni D, Renaud B, Chouvet G (2002) The switch of subthalamic neurons from an irregular to a bursting pattern does not solely depend on their GABAergic inputs in the anesthetic-free rat. J Neurosci 22:8665-8675.
[22] Harris KD, Hirase H, Leinekugel X, Henze DA, Buzsáki G (2001) Temporal interaction between single spikes and complex spike bursts in hippocampal pyramidal cells. Neuron 32:141-149.
[23] Barker JL, Gainer H (1975) Studies on bursting pacemaker potential activity in molluscan neurons. I. Membrane properties and ionic contributions. Brain Res 84:461-477.
[24] Jahnsen H, Llinas R (1984) Ionic basis for the electroresponsiveness and oscillatory properties of guinea-pig thalamic neurones *in vitro*. J Physiol (Lond) 349:227-247.
[25] Gray CM, McCormick DA (1996) Chattering cells: Superficial pyramidal neurons contributing to the generation of synchronous firing in the visual cortex. Science 274:109-113.
[26] Legéndy CR, Salcman M (1985) Bursts and recurrences of bursts in the spike trains of spontaneously active striate cortex neurons. J Neurophysiol 53:926-939.
[27] Bair W, Koch C, Newsome W, Britten K (1994) Power spectrum analysis of bursting cells in area MT in the behaving monkey. J Neurosci 14:2870-2892.
[28] Snider RK, Kabara JF, Roig BR, Bonds AB (1998) Burst firing and modulation of functional connectivity in cat striate cortex. J Neurophysiol 80:730-744.

[29] Wang X-J (1999) Fast burst firing and short-term synaptic plasticity: a model of neocortical chattering neurons. Neuroscience 89:347-362.
[30] Williams SR, Stuart GJ (1999) Mechanisms and consequences of action potential burst firing in rat neocortical pyramidal neurons. J Physiol (London) 521:467-482.
[31] Swadlow HA, Gusev AG (2001) The impact of 'bursting' thalamic impulses at a neocortical synapse. Nature Neurosci 4:402-408.
[32] Goense JBM, Ratnam R, Nelson ME (in press) Burst firing improves the detection of weak signals in spike trains. Neurocomp
[33] Guido W, Lu SM, Vaughan JW, Godwin DW, Sherman SM (1995) Receiver operating characteristic (ROC) analysis of neurons in the cat's lateral geniculate nucleus during tonic and burst response mode. Visual Neuroscience 12:723-41.
[34] Eggermont JJ, Smith GM (1996) Burst-firing sharpens frequency-tuning in primary auditory cortex. Neuroreport 7:753-7.
[35] Bastian J (2003) Electrolocation. In: The handbook of brain theory and neural networks. 2nd ed. (Arbib MA, ed), pp 391-394. Cambridge, MA: MIT Press.
[36] Turner RW, Maler L, Burrows M (1999) Electrolocation and electrocommunication. J Exp Biol 202
[37] Konishi M (1990) Similar algorithms in different sensory systems and animals. Cold Spring Harb Symp Quant Biol 55:575-584.
[38] Konishi M (1991) Deciphering the brain's codes. Neural Comput 3:1-18.
[39] Carr CE, Friedman MA (1999) Evolution of time coding systems. Neural Comput 11:1-20.
[40] Kaas JH (1997) Topographic maps are fundamental to sensory processing. Brain Res Bull 44:107-12.
[41] Sillito AM, Jones HE, Gerstein GL, West DC (1994) Feature-linked synchronization of thalamic relay cell firing induced by feedback from the visual cortex. Nature 369:479-82.
[42] Destexhe A (2000) Modelling corticothalamic feedback and the gating of the thalamus by the cerebral cortex. Journal of Physiology (Paris) 94:391-410.
[43] Kalmijn J (1982) Electric and magnetic field detection in elasmobranch fishes. Science 218:916-918.
[44] Moller P (1995) Electric fishes. History and behavior. Fish and Fisheries Series, vol 17 (Pitcher TJ, ed) London: Chapman and Hall.
[45] Assad C, Rasnow B, Stoddard PK (1999) The electric organ discharges and electric images during electrolocation. J Exp Biol 202:1185-1193.
[46] Nelson ME, MacIver MA (1999) Prey capture in the weakly electric fish *Apteronotus albifrons*: Sensory acquisition strategies and electrosensory consequences. J Exp Biol 202:1195–1203.

[47] Nelson ME, MacIver MA, Coombs S (2002) Modeling electrosensory and mechanosensory images during the predatory behavior of weakly electric fish. Brain Behav Evol 59:199-210.
[48] Hagedorn M, Heiligenberg W (1985) Court and spark: electric signals in the courtship and mating of gymnotoid electric fish. Anim Behav 33:254-265.
[49] Hopkins CD (1988) Neuroethology of electric communication. Annu Rev Neurosci 11:497-535.
[50] Metzner W, Viete S (1996) The neuronal basis of communication and orientation in the weakly electric fish, *Eigenmannia*. I. Communication behavior or: Seeking a conspecific's response. Naturwissenschaften 83:6-14.
[51] Scheich H, Bullock TH, Hamstra RHJ (1973) Coding properties of two classes of afferent nerve fibers: high frequency electroreceptors in the electric fish, *Eigenmannia*. J Neurophysiol 36:39-60.
[52] Carr CE, Maler L, Sas E (1982) Peripheral organization and central projections of the electrosensory nerves in gymnotiform fish. J Comp Neurol 211:139-153.
[53] Heiligenberg W, Dye J (1982) Labeling of electroreceptive afferents in a gymnotoid fish by intracellular injection of HRP: the mystery of multiple maps. J Comp Physiol A 148:287-296.
[54] Maler L, Sas EK, Rogers J (1981) The cytology of the posterior lateral line lobe of high-frequency weakly electric fish (Gymnotidae): dendritic differentiation and synaptic specificity in a simple cortex. J Comp Neurol 195:87-139.
[55] Saunders J, Bastian J (1984) The physiology and morphology of two types of electrosensory neurons in the weakly electric fish, *Apteronotus leptorhynchus*. J Comp Physiol A 154:199-209.
[56] Bastian J (1981a) Electrolocation. II. The effects of moving objects and other electrical stimuli on the activities of two categories of posterior lateral line lobe cells in *Apteronotus albifrons*. J Comp Physiol A 144:481-494.
[57] Shumway C (1989a) Multiple electrosensory maps in the medulla of weakly electric gymnotiform fish. I. Physiological differences. J Neurosci 9:4388-4399.
[58] Bastian J, Chacron MJ, Maler L (2002) Receptive field organization determines pyramidal cell stimulus-encoding capability and spatial stimulus selectivity. J Neurosci 22:4577-4590.
[59] Bastian J (1999) Plasiticity of feedback inputs in the apteronotid electrosensory system. J Exp Biol 202:1327-1337.
[60] Berman NJ, Maler L (1999) Neural architecture of the electrosensory lateral line lobe: Adaptations for coincidence detection, a sensory searchlight and frequency-dependent adaptive filtering. J Exp Biol 202:1243-1253.

[61] Bell CC (2001) Memory-based expectations in electrosensory systems. Curr Opin Neurobiol 11:481-487.
[62] Doiron B, Chacron MJ, Maler L, Longtin A, Bastian J (2003) Inhibitory feedback required for network oscillatory responses to communication but not prey stimuli. Nature 421:539-543.
[63] Bastian J (1981b) Electrolocation. I. How the electroreceptors of *Apteronotus albifrons* code for moving objects and other electrical stimuli. J Comp Physiol A 144:465-479.
[64] Xu Z, Payne JR, Nelson ME (1996) Logarithmic time course of sensory adaptation in electrosensory afferent nerve fibers in a weakly electric fish. J Neurophysiol 76:2020-2032.
[65] Nelson ME, Xu Z, Payne JR (1997) Characterization and modeling of P-type electrosensory afferent responses to amplitude modulations in a wave-type electric fish. J Comp Physiol A 181:532-544.
[66] Ratnam R, Nelson ME (2000) Nonrenewal statistics of electrosensory afferent spike trains: implications for the detection of weak sensory signals. J Neurosci 20:6672-6683.
[67] Wessel R, Koch C, Gabbiani F (1996) Coding of time-varying electric field amplitude modulations in a wave-type electric fish. J Neurophysiol 75:2280-2293.
[68] Kreiman G, Krahe R, Metzner W, Koch C, Gabbiani F (2000) Robustness and variability of neuronal coding by amplitude-sensitive afferents in the weakly electric fish *Eigenmannia*. J Neurophysiol 84:189-204.
[69] Chacron MJ, Longtin A, Maler L (2001) Negative interspike interval correlations increase the neuronal capacity for encoding time-dependent stimuli. J Neurosci 21:5328-5343.
[70] Shumway C (1989b) Multiple electrosensory maps in the medulla of weakly electric gymnotiform fish. II. Anatomical differences. J Neurosci 9:4400-4415.
[71] Krahe R, Kreiman G, Gabbiani F, Koch C, Metzner W (2002) Stimulus encoding and feature extraction by multiple sensory neurons. J Neurosci 22:2374-2382.
[72] Gabbiani F, Metzner W (1999) Encoding and processing of sensory information in neural spike trains. J Exp Biol 202:1267-1279.
[73] Heiligenberg W (1991) Neural nets in electric fish. Cambridge, MA: MIT Press.
[74] Lehky SR, Sejnowski TJ, Desimone R (1992) Predicting responses of nonlinear neurons in monkey striate cortex to complex paterns. J Neurosci 12:3568-3581.
[75] Green DM, Swets JA (1966) Signal detection theory and psychophysics. New York, NY: Wiley.
[76] Gabbiani F, Koch C (1998) Principles of spike train analysis. In: Methods in neuronal modeling (Koch C, Segev I, eds), pp 313-360. Cambridge, MA: MIT Press.

[77] Krahe R, Kreiman G, Gabbiani F, Koch C, Metzner W (in prep.) Feature extraction from global and local stimuli by electrosensory neurons.
[78] Metzner W, Juranek J (1997) A sensory brain map for each behavior. Proc Natl Acad Sci USA 94:14798-14803.
[79] Sherman SM (2001b) A wake-up call from the thalamus. Nature Neurosci 4:344-346.
[80] Steriade M (2001) To burst, or rather, not to burst. Nature Neurosci 4:671.
[81] Swadlow HA, Gusev AG, Bezdudnaya T (2002) Activation of a cortical column by a thalamocortical impulse. J Neurosci 22:7766-7773.
[82] Sherman SM (1996) Dual response modes in lateral geniculate neurons: mechanisms and functions. Vis Neurosci 13:205-13.
[83] Chagnac-Amitai Y, Luhmann HJ, Prince DA (1990) Burst generating and regular spiking layer 5 pyramidal neurons of rat neocortex have different morphological features. J Comp Neurol 296:598-613.
[84] Connors BW, Gutnick MJ (1990) Intrinsic firing patterns of diverse neocortical neurons. Trends Neurosci 13:99-104.
[85] Mason A, Larkman A (1990) Correlations between morphology and electrophysiology of pyramidal neurons in slices of rat visual cortex. II. Electrophysiology. J Neurosci 10:1415-1428.
[86] Mainen ZF, Sejnowski TJ (1996) Influence of dendritic structure on firing pattern in model neocortical neurons. Nature 382:363-366.
[87] Bastian J, Courtright J (1991) Morphological correlates of pyramidal cell adaptation rate in the electrosensory lateral line lobe of weakly electric fish. J Comp Physiol A 168:393-407.
[88] Turner RW, Maler L (1999) Oscillatory and burst discharge in the Apteronotid electrosensory lateral line lobe. J Exp Biol 202:1255-1265.
[89] Turner RW, Plant JR, Maler L (1996) Oscillatory and burst discharges across electrosensory topographic maps. J Neurophysiol 76:2364-2382.
[90] Turner RW, Maler L, Deerinck T, Levinson SR, Ellisman MH (1994) TTX-sensitive dendritic sodium channels underlie oscillatory discharge in a vertebrate sensory neuron. J Neurosci 14:6453-6471.
[91] Häusser M, Spruston N, Stuart GJ (2000) Diversity and dynamics of dendritic signaling. Science 290:739-744.
[92] Lemon N, Turner RW (2000) Conditional spike backpropagation generates burst discharge in a sensory neuron. J Neurophysiol 84:1519-1530.
[93] Rashid AJ, Dunn RJ, Turner RW (2001) A prominent soma-dendritic distribution of Kv3.3 $K^+$ channels in electrosensory and cerebellar neurons. J Comp Neurol 441:234-247.
[94] Rashid AJ, Morales E, Turner RW, Dunn RJ (2001) The contribution of dendritic Kv3 $K^+$ channels to burst threshold in a sensory neuron. J Neurosci 21:125-135.

[95] Noonan L, Doiron B, Laing C, Longtin A, Turner RW (in press) A dynamic dendritic refractory period regulates burst discharge in the electrosensory lobe of weakly electric fish. J Neurosci.
[96] Doiron B, Noonan L, Lemon N, Turner RW (2003) Persistent $Na^+$ current modifies burst discharge by regulating conditional backpropagation of dendritic spikes. J Neurophysiol 89:324-337.
[97] Huguenard JR (1996) Low-threshold calcium currents in central nervous system neurons. Annu Rev Physiol 58:329-348.
[98] Rhodes PA, Gray CM (1994) Simulations of intrinsically bursting pyramidal neurons. Neural Comput 6:1086-1110.
[99] Berman NJ, Plant J, Turner RW, Maler L (1997) Excitatory amino acid receptors at a feedback pathway in the electrosensory system: implications for the searchlight hypothesis. J Neurophysiol 78:1869-1881.
[100] Doiron B, Longtin A, Turner RW, Maler L (2001) Model of gamma frequency burst discharge generated by conditional backpropagation. J Neurophysiol 86:1523-1545.
[101] Berman NJ, Dunn RJ, Maler L (2001) Function of NMDA receptors and persistent sodium channels in a feedback pathway of the electrosensory system. J Neurophysiol 86:1612-1621.
[102] Rinzel J, Ermentrout B (1998) Analysis of neural excitability and oscillations. In: Methods in neuronal modeling (Koch C, Segev I, eds), pp 251-291. Cambridge, MA: MIT Press.
[103] Doiron B, Laing C, Longtin A, Maler L (2002) Ghost bursting: a novel neuronal burst mechanism. J Comput Neurosci 12:5-25.
[104] Laing CR, Longtin A (2002) A two-variable model of somatic-dendritic interactions in a bursting neuron. Bull Math Biol 64:829-860.
[105] Kepecs A, Wang X-J (2000) Analysis of complex bursting in cortical pyramidal neuron models. Neurocomp 32-33:181-187.
[106] Hodgkin AL, Huxley AF (1952) A quantitative description of membrane currents and its application to conduction and excitation in nerve. J Physiol (London) 117:500-544.
[107] Izhikevich EM (2000) Neural excitabilty, spiking and bursting. Int J Bifn Chaos 10:1171-1266.
[108] Strogatz SH (1994) Nonlinear dynamics and chaos with applications to physics, biology, chemistry, and engineering. Reading, MA: Addison-Wesley.
[109] Bal T, Nagy F, Moulins M (1988) The pyloric central pattern generator in crustacea: a set of conditional neuronal oscillators. J Comp Physiol A 163:715-727.
[110] Grillner S, Ekeberg Ö, El Manira A, Lansner A, Parker D, Tegner J, Wallen P (1998) Intrinsic function of a neuronal network - a vertebrate central pattern generator. Brain Res Rev 26:184-197.

[111] Amir R, Michaelis M, Devor M (2002) Burst discharge in primary sensory neurons: triggered by subthreshold oscillations, maintained by depolarizing afterpotentials. J Neurosci 22:1187-1198.
[112] Larkman A, Mason A (1990) Correlations between morphology and electrophysiology of pyramidal neurons in slices of rat visual cortex. I. Establishment of cell classes. J Neurosci 10:1407-1414.
[113] Schwindt P, Crill W (1999) Mechanisms underlying burst and regular spiking evoked by dendritic depolarization in layer 5 cortical pyramidal neurons. J Neurophysiol 81:1341-1354.
[114] Jung H-Y, Staff NP, Spruston N (2001) Action potential bursting in subicular pyramidal neurons is driven by a calcium tail current. J Neurosci 21:3312-3321.
[115] Golding NL, Jung H-Y, Mickus T, Spruston N (1999) Dendritic calcium spike initiation and repolarization are controlled by distinct potassium channel subtypes in CA1 pyramidal neurons. J Neurosci 19:8789-8798.
[116] Magee JC, Carruth M (1999) Dendritic voltage-gated ion channels regulate the action potential firing mode of hippocampal CA1 pyramidal neurons. J Neurophysiol 82:1895-1901.
[117] Brumberg JC, Nowak LG, McCormick DA (2000) Ionic mechanisms underlying repetitive high-frequency burst firing in supragranular cortical neurons. J Neurosci 20:4829-4843.
[118] Nishimura Y, Asahli M, Saitoh K, Kitagawa H, Kumazawa Y, Itoh K, Lin M, Akamine T, Shibuya H, Asahara T, Yamamoto T (2001) Ionic mechanisms underlying burst firing of layer III sensorimotor cortical neurons of the cat: an *in vitro* slice study. J Neurophysiol 86:771-781.
[119] Azouz R, Jensen MS, Yaari Y (1996) Ionic basis for spike after-depolarization and burst generation in adult rat hippocampal CA1 pyramidal cells. J Physiol (London) 492:211-223.
[120] Su H, Alroy G, Kirson ED, Yaari Y (2001) Extracellular calcium modulates persistent sodium current-dependent burst-firing in hippocampal pyramidal neurons. J Neurosci 21:4173-4182.
[121] Steriade M, Timofeev I, Dürmüller N, Grenier F (1998) Dynamic properties of corticothalamic neurons and local cortical interneurons generating fast rhythmic (30-40 Hz) spike bursts. J Neurophysiol 79:483-490.
[122] Destexhe A, Neubig M, Ulrich D, Huguenard J (1998) Dendritic low-threshold calcium currents in thalamic relay cells. J Neurosci 18:3574-3588.
[123] D'Angelo E, Nieus T, Maffei A, Armano S, Rossi P, Taglietti V, Fontana A, Naldi G (2001) Theta-frequency bursting and resonance in cerebellar granule cells: experimental evidence and modeling of a slow- $K^+$-dependent mechanism. J Neurosci 21:759-770.
[124] Silva LR, Amitai Y, Connors BW (1991) Intrinsic oscillations of neocortex generated by layer 5 pyramidal neurons. Science 251:432-435.

[125] Falcke M, Huerta R, Rabinovich MI, Abarbanel HDI, Elson RC, Selverston AI (2000) Modeling observed chaotic oscillations in bursting neurons: the role of calcium dynamics and $IP_3$. Biol Cybern 82:517-527.
[126] Spruston N, Schiller Y, Stuart G, Sakmann B (1995) Activity-dependent action potential invasion and calcium influx into hippocampal CA1 pyramidal cells. Science 268:297-300.
[127] Colbert CM, Magee JC, Hoffman DA, Johnston D (1997) Slow recovery from inactivation of $Na^+$ channels underlies the activity-dependent attentuation of dendritic action potentials in hippocampal CA1 pyramidal neurons. J Neurosci 17:6512-6521.
[128] Buzsáki G, Penttonen M, Nadasdy Z, Bragin A (1996) Pattern- and inhibition-dependent invasion of pyramidal cell dendrites by fast spikes in the hippocampus *in vivo*. Proc Natl Acad Sci USA 93:9921-9925.
[129] Tsubokawa H, Ross WN (1996) IPSPs modulate spike backpropagation and associated $[Ca^{2+}]$ changes in the dendrites of hippocampal CA1 pyramidal neurons. J Neurophysiol 76:2896-2906.
[130] Lowe G (2002) Inhibition of backpropagating action potentials in mitral cell secondary dendrites. J Neurophysiol 88:64-85.
[131] Kepecs A, Wang X-J, Lisman J (2002) Bursting neurons signal input slope. J Neurosci 22:9053-9062.
[132] Segev I, Rall W (1998) Excitable dendrites and spines: earlier theoretical insights elucidate recent direct observations. Trends Neurosci 21:453-460.
[133] Brandman R, Nelson ME (2002) A simple model of long-term spike train regularization. Neural Comput 14:1575-1597.

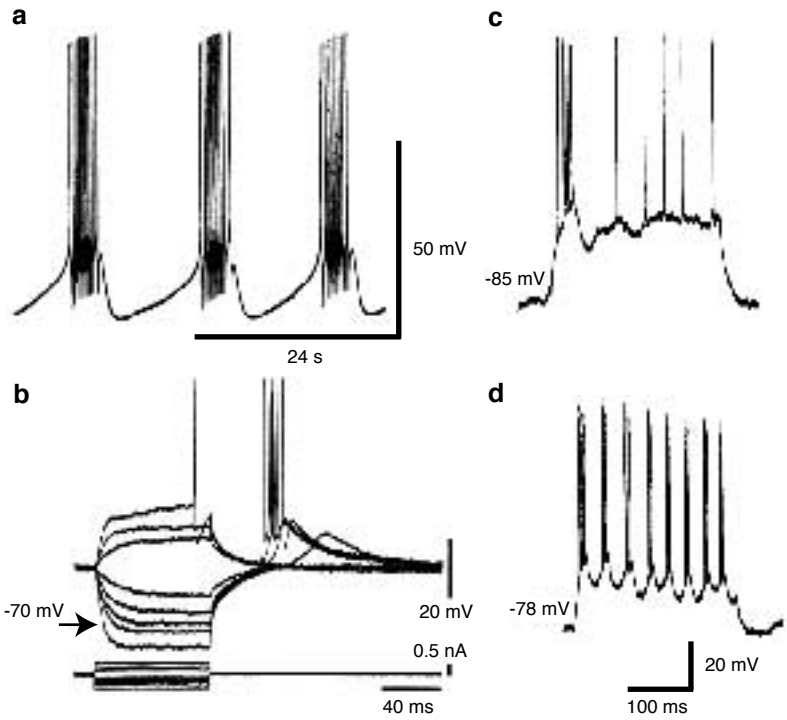


Krahe and Gabbiani: Figure 1

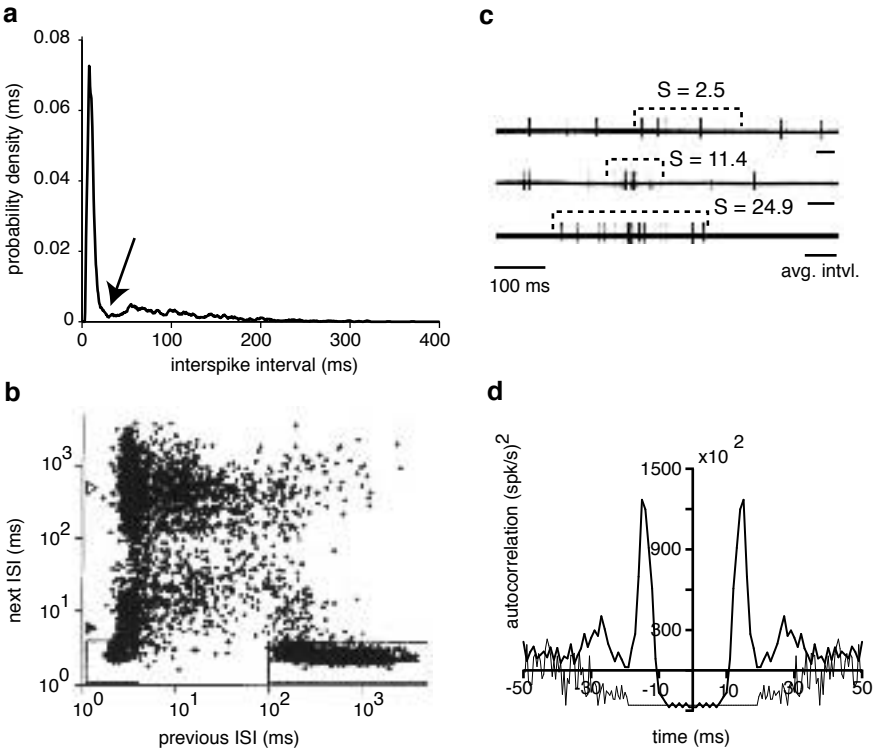


Krahe and Gabbiani: Figure 2

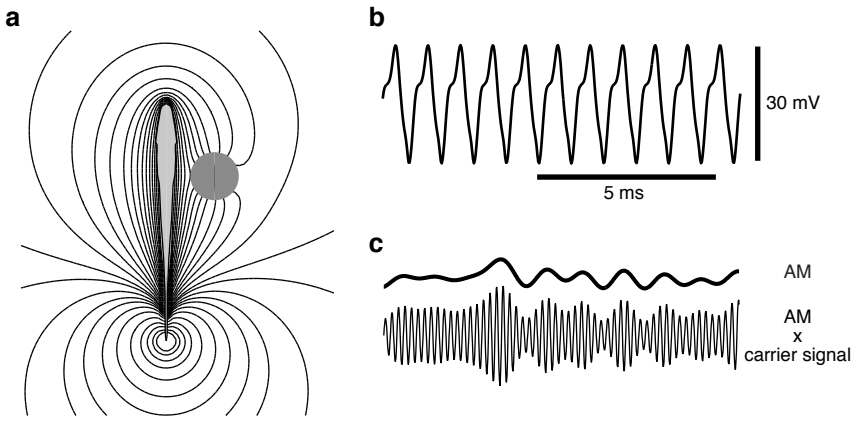


Krahe and Gabbiani: Figure 3

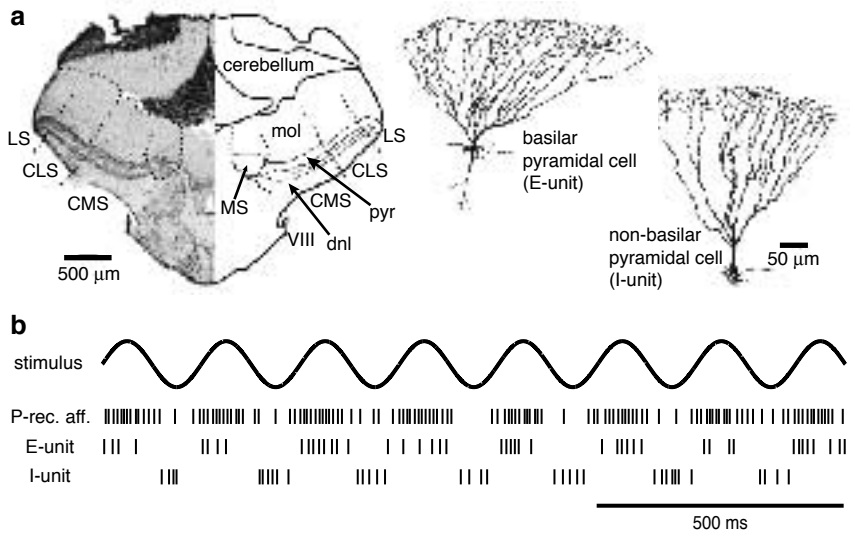


Krahe and Gabbiani: Figure 4

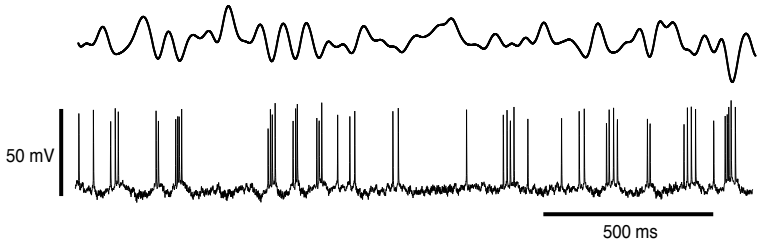


Krahe and Gabbiani: Figure 5

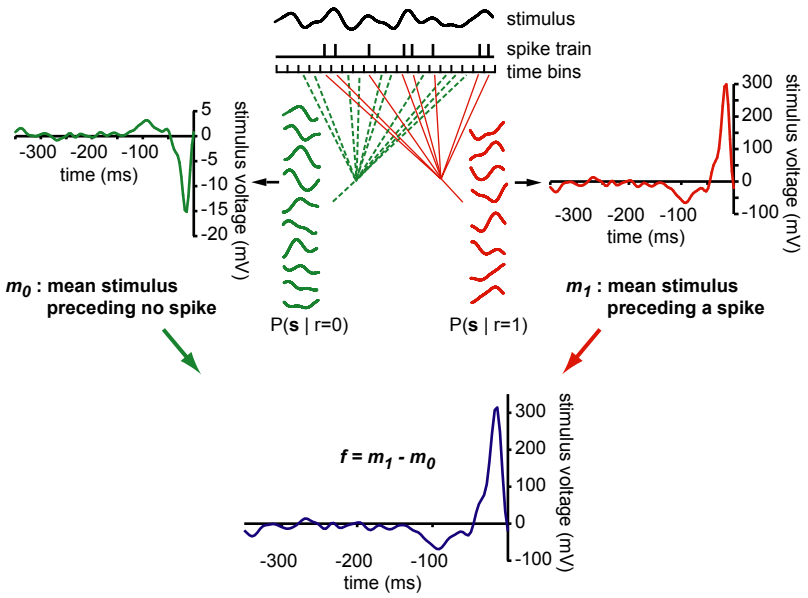


Krahe and Gabbiani: Figure 6

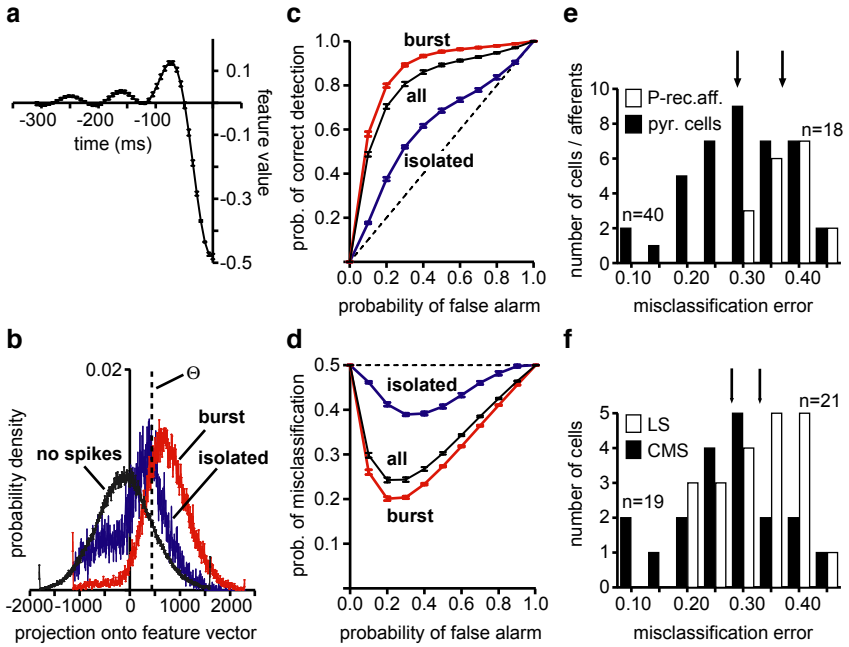


Krahe and Gabbiani: Figure 7

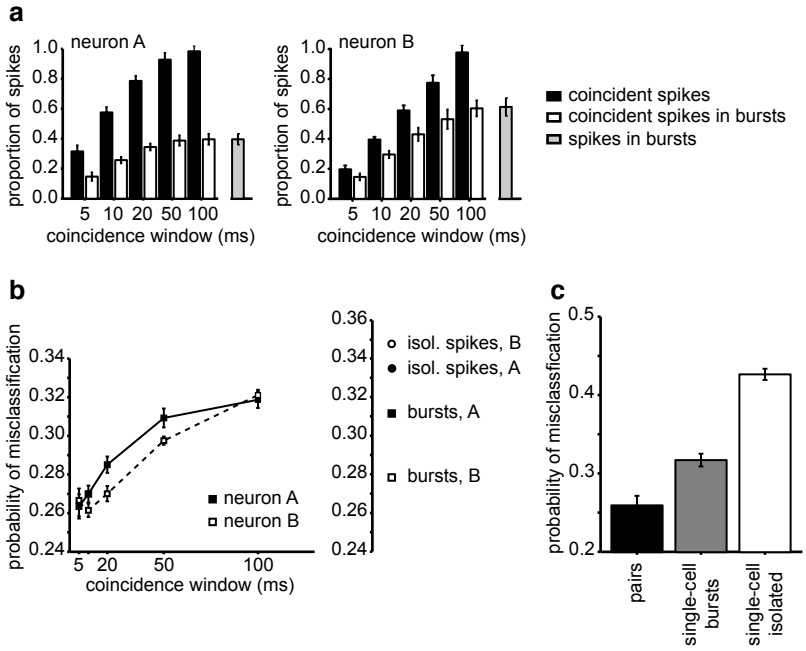


Krahe and Gabbiani: Figure 8

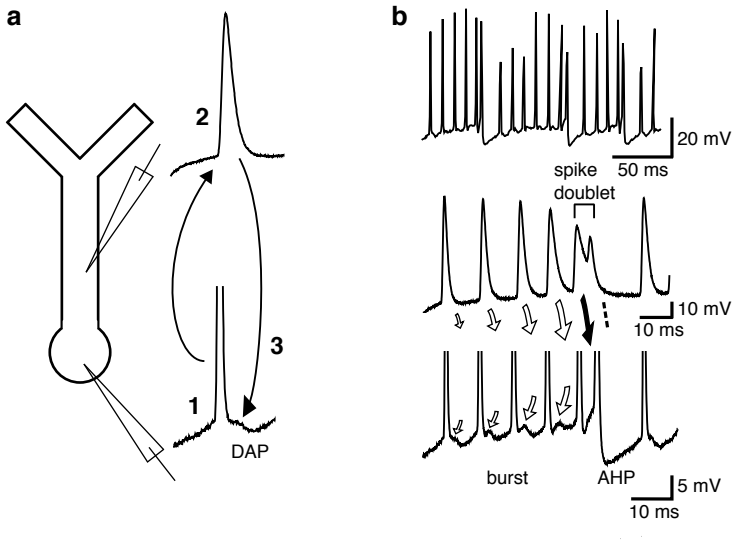


caption: sources

Krahe and Gabbiani: Figure 9

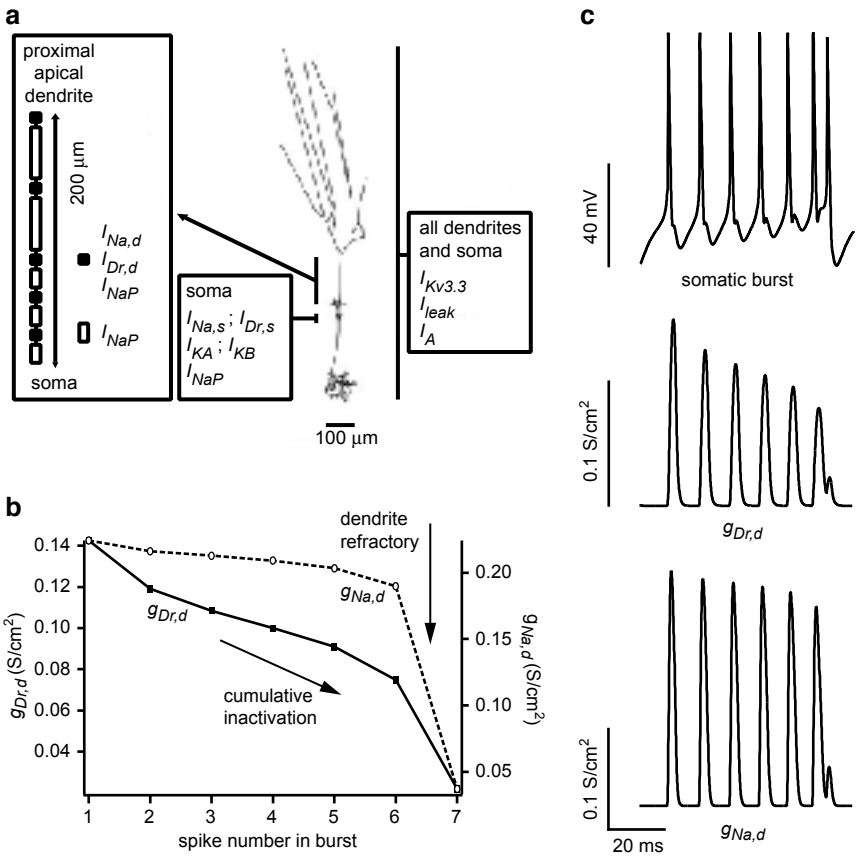


Krahe and Gabbiani: Figure 10

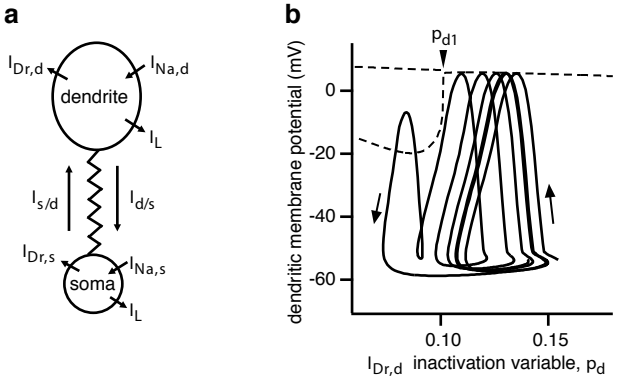


Krahe and Gabbiani: Figure 11

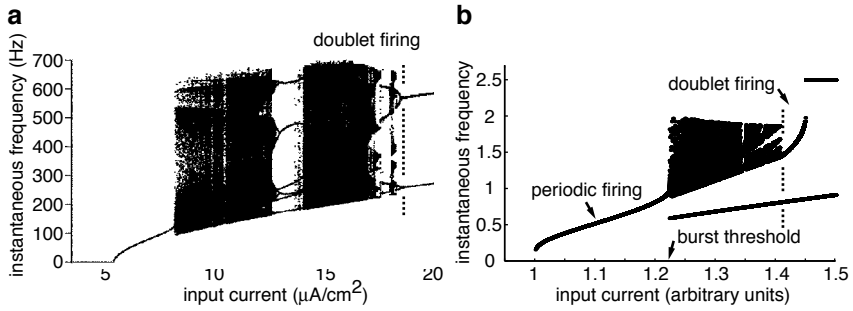


Krahe and Gabbiani: Figure 12